

PVT Measurements on Tetrafluoroethane (R134a) Along the Vapor–Liquid Equilibrium Boundary Between 288 and 373 K and in the Liquid State from the Triple Point to 265 K¹

W. Blanke,² G. Klingenberg,^{2,3} and R. Weiss²

For the investigations of the gas–liquid phase equilibria, a new apparatus has been developed capable of simultaneously determining the pressure and the liquid and vapor densities using Archimedes' principle. The relative measurement uncertainties of the liquid and vapor densities of R134a (purity, 99.999%) at 313 K are 2×10^{-4} and 7×10^{-4} , respectively (95% confidence level). For the measurements in the liquid region along nine quasi-isochores at pressures up to 5 MPa, an isochoric apparatus was used. The relative measurement uncertainty of $pv/(RT)$ is less than 1×10^{-3} . In addition to the investigation of the (p, v, T) properties, the temperature and pressure at the triple point and the vapor pressure between the triple point and 265 K were measured. On the basis of these data, a vapor pressure correlation has been developed that reproduces the measured vapor pressures within the uncertainty of measurement. The results of our measurements are compared with a fundamental equation for R134a, which is based on the measurements of other research groups.

KEY WORDS: Archimedes' principle; gas–liquid phase equilibrium; isochores; triple point; vapor pressure.

1. INTRODUCTION

For the determination of equations of state, high-accuracy measurements of the saturated liquid and saturated vapor densities and the saturation pressure and temperature are required. A new apparatus has therefore

¹ Paper presented at the Twelfth Symposium on Thermophysical Properties, June 19–24, 1994, Boulder, Colorado, U.S.A.

² Physikalisch-Technische Bundesanstalt, Bundesallee 100, D-38116 Braunschweig, Germany.

³ To whom correspondence should be addressed.

been constructed based on Archimedes' principle. To test the apparatus, properties of the well-known alternative refrigerant R134a [1–10] were measured on the vapor–liquid equilibrium boundary. In addition, (pvT) measurements were carried out in the single-phase liquid region. The results are compared with equations given by Tillner-Roth [2].

2. EXPERIMENTS

2.1. Saturation Pressure and Densities

The experimental apparatus consists of components and instrumentation for measurement of saturation densities, adjustment and measurement of the saturation pressure, and temperature stabilization and measurement. A schematic diagram of the apparatus is given in Fig. 1. The main components are a microbalance, a magnetic suspension coupling, and a sinker. An AT 261 microbalance with a resolution of 0.01 mg, manufactured by Mettler (Switzerland), is mounted above the magnetic coupling manufactured by Rubotherm (Germany). A detailed description of the coupling is given by Wagner et al. [11].

The principle of operation is as follows. An electromagnet is fixed at the bottom load hook of the balance. This is connected to the electronic unit via two Pt–Ir wires of only 0.1 mm in diameter. The electromagnet is separated from the permanent, suspended magnet by a diamagnetic copper–beryllium disk, forming the upper part of the pressure vessel. The permanent magnet

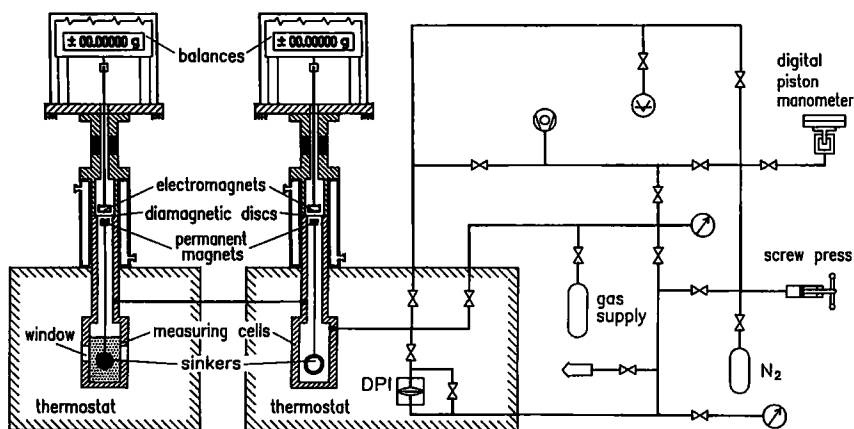


Fig. 1. Schematic diagram of the new apparatus for (p, ρ', ρ'', T) measurements along the gas–liquid saturation curve.

is encased in a stainless-steel housing, which is welded to a rod carrying a sensing element and the sinker support. Using the signal of this position-indicating sensor, the electronic unit changes the distance between the electromagnet and the permanent magnet until the dc current in the electromagnet is zero. The power consumption of the electromagnet is therefore low. The suspension coupling has the advantage of two stable positions. In this lower position only the permanent magnet with the rod and one part of the sinker support are suspended. In the upper position, the rest of the support and the sinker are also suspended. At every point of measurement, the balance containing the weight of the permanent magnet without the sinker is tared. Then the internal calibration of the balance is performed and the weight of the sinker is added by selecting the upper suspension position. This procedure is used to avoid a zero drift of the electronic balance. The stability of the balances including the couplings was tested over a one-month period. During this time a very good long-term stability, $\Delta m/m < 5 \times 10^{-5}$, at room temperature and atmospheric pressure was observed.

The density of the fluid is given by the simple equation

$$\rho = [m_s - m(1 - \rho_a/\rho_n) + m_{su}(1 - \rho_g/\rho_n)]/V \quad (1)$$

where ρ_a , ρ_g , and ρ_n are the density of the ambient air, the pressurized gas under investigation, and the reference weights ($8000 \text{ kg} \cdot \text{m}^{-3}$), respectively; m , the balance reading; m_s and m_{su} , the mass of the sinker and of that part of the support suspended with the sinker; and V , the volume of the sinker. The gas density, ρ_g , is calculated from equations given by Tillner-Roth [1]. The volume of the sinkers made of quartz glass depends on pressure and temperature. The cubic expansion coefficient, $1.5 \times 10^{-6} \text{ K}^{-1}$, is very small. The sinker for the measurement in the liquid phase is a solid sphere with a volume of $(10.64403 \pm 0.0005) \text{ cm}^3$ and a mass of $(23.43734 \pm 0.0001) \text{ g}$. The confidence level is 95%. The hollow sinker for the gas was designed for a density of approximately $1000 \text{ kg} \cdot \text{m}^{-3}$, since nearly all gases at the critical point have lower densities than $1000 \text{ kg} \cdot \text{m}^{-3}$. An additional contribution to the measurement uncertainty is made by the unknown pressure in the hollow sphere which is assumed to be smaller than the ambient pressure. The elastic distortion coefficients of the two sinkers calculated from elastic theory are fairly similar: 3.1×10^{-5} and $2.7 \times 10^{-5} \text{ MPa}^{-1}$.

The two balances are mounted side by side on a common base plate at a distance of 9 cm, sufficient to avoid electromagnetic interferences. Below the suspension couplings, lengthening tubes and measuring cells are installed. The cell for the liquid density measurement is equipped with

a window, enabling the meniscus to be observed directly during the measurements. Each cell is immersed in a bath thermostat. The thermostat for the gas density measurement is always kept at a temperature 0.3 K higher than that for the liquid to avoid condensation. The vapor density is extrapolated to the saturated vapor density using Eq. B15 [1]. The suspension couplings and the lengthening tubes are thermostatted a few kelvins above the temperature of the fluid. The connecting tube between the two cells is electrically heated. The temperature of the cells is measured by means of carefully calibrated Pt 25- Ω resistance thermometers, a Senator resistance bridge, manufactured by Tinsley (UK), a standard resistor, and a programmable switch from Keithley (USA). With this equipment, it is possible to measure T_{90} in the range from 234 to 430 K with a standard deviation of 1 mK. The stability of the thermostats limits the uncertainty of the temperature of the fluid. For the vapor pressure measurement, a direct-indicator gauge piston manometer with a load cell manufactured by Desgranges & Huot (France) together with a differential pressure indicator from Ruska (USA) and a digital barometer from Setra (USA) are used. The piston gauge with a measuring range of 8 MPa has a resolution of 50,000 digits/MPa. It was calibrated before and after the measurement series. The differential pressure cell is used as a null indicator for separating the gas under investigation from nitrogen, the pressure-transmitting medium. Before starting the measurements, the null indicator was calibrated with nitrogen at several different temperatures and line pressures. Since care was taken to avoid mechanical stresses from the null indicator due to tubing, good repeatability was achieved. The estimated standard deviation of the whole pressure measuring chain, including the barometer, is

$$u = [(0.2 \text{ kPa})^2 + (4 \times 10^{-5} p)^2]^{-1/2} \quad (2)$$

Here the head corrections of the nitrogen and the gas under investigation are not yet taken into account. To get reliable head corrections, six Pt 100- Ω resistance thermometers are installed along the tubing. A scanning digital multimeter from Prema (Germany) is used to measure the corresponding resistances, and also those from thermometers for the ambient temperature and the piston manometer, and the dc output of the null indicator.

Before starting the filling procedure, the apparatus was helium leak-tested and evacuated over a period of 2 days using a turbomolecular pump. The densitometer for the measurement of the liquid phase was then cooled down and R134a of a high purity (99.999%) was condensed into this cell. Before starting the measurement, it was necessary to adjust the nitrogen pressure by changing the volume until the null indicator showed zero differential pressure. The

balances were then tared, and their internal calibration routine was started. After calibration, the suspension couplings were switched to the upper position and the computer program for collecting the data was started.

2.2. Quasi-Isochores in the Liquid Single-Phase Region

In the liquid region of state, which was investigated, an isochoric apparatus was used, which has already been described elsewhere [12]. The relative uncertainty of measurement, related to $pv/(RT)$, is less than 1×10^{-3} . Measurements on nine quasi-isochores were carried out from the triple point to 265 K at pressures up to 5 MPa.

2.3. Triple Point and Vapor Pressure up to 265 K

For the determination of the triple point, an adiabatic method was used. With this method, triple points as well as vapor pressures can be determined. Details regarding the construction and operation of the equipment are given in Refs. 12 and 13.

3. RESULTS

The experimental results for the (p, ρ', ρ'', T) properties of R134a are given in Table I. The results are compared with the fundamental equation given by Tillner-Roth and Baehr [2], based on their own measurements and the measurements of other research groups. The relative deviation of the vapor pressure from the fundamental equation shows a systematic deviation of about 1×10^{-3} . The relative deviation of the saturated liquid density from the fundamental equation is shown in Fig. 2. The maximum deviation, measured 1 K below the critical temperature, is 6×10^{-3} . In addition in Fig. 2, the relative deviation of the vapor density from the fundamental equation is plotted. All the differences are smaller than 4×10^{-3} apart from those at about 372 K.

In the uncertainty analysis, the following effects were ignored: adsorption, convection, surface tension, and the temperature dependence of the diamagnetism of the copper-beryllium disk and of the magnetization of the permanent magnet and the electromagnet. At 313 K, the uncertainty of the saturated liquid density was estimated to be $0.19 \text{ kg} \cdot \text{m}^{-3}$, and that of the vapor density $0.035 \text{ kg} \cdot \text{m}^{-3}$.

The (pvT) data measured in the single-phase liquid region are listed in Table II. The fundamental equation of Tillner-Roth [2] represents the measured densities also at low temperatures within the uncertainty of measurements of $10^{-3} \rho$.

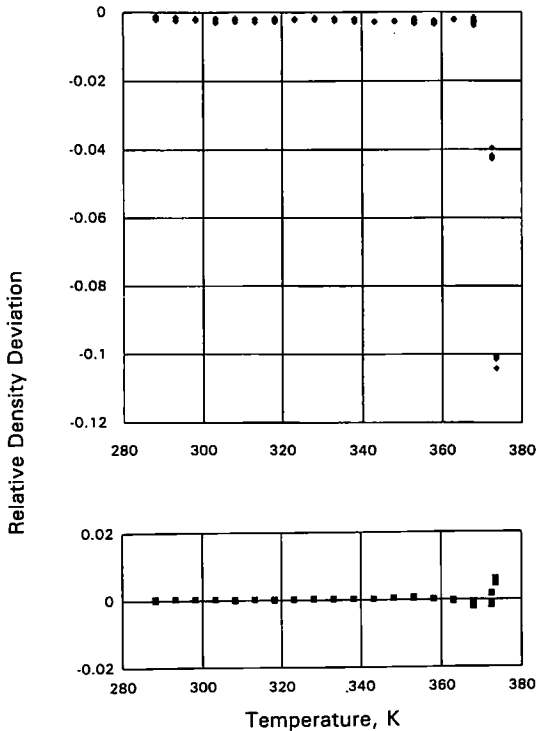


Fig. 2. Relative deviations $(\rho_{\text{meas}} - \rho_{\text{cal}})/\rho_{\text{cal}}$ of measured densities from densities calculated with the fundamental equation of Tillner-Roth and Baehr [2]. (■) Liquid; (◆) vapor.

The results of the vapor pressure measurements at temperatures between 175 and 280 K are given in Table III. The deviations of values calculated with the fundamental equation [2] are shown in Fig. 3. For the correlation of the measured pressure-temperature values an approach was used which had been suggested by Wagner [14].

$$\ln(p_s/p_{cr}) = (T_{cr}/T)(A\tau + B\tau^{1.5} + C\tau^{2.5} + D\tau^5) \quad (3)$$

where $\tau = 1 - T/T_{cr}$.

The critical parameters T_{cr} and p_{cr} were taken from Ref. 2. They are listed in Table III along with the measured values and the coefficients of Eq. (3). For the triple point we found the plateau temperature of $T_{tp} = (169.861 \pm 0.005)$ K. The corresponding pressure is $p_{tp} = (0.42 \pm 0.01)$ kPa.

Table I. p v T Data of R134a in the Saturated State

T_{00} (K)	p (MPa)	ρ' ($\text{kg} \cdot \text{dm}^{-3}$)	ρ'' ($\text{kg} \cdot \text{dm}^{-3}$)
288.254	048976	1.24345	0.023800
293.228	0.57262	1.22546	0.027791
298.176	0.66528	1.20698	0.032308
303.188	0.77043	1.18762	0.037491
308.176	0.88692	1.16764	0.043350
313.165	1.01607	1.14691	0.049983
318.145	1.15875	1.12527	0.057531
323.168	1.31717	1.10244	0.066169
328.139	1.48963	1.07861	0.075931
333.135	1.67933	1.05320	0.087161
338.126	1.88669	1.02608	0.100108
343.106	2.11185	0.99685	0.115106
348.089	2.35797	0.96492	0.132901
353.087	2.62566	0.92936	0.154277
318.179	1.15970	1.12493	0.057561
288.288	0.49026	1.24278	0.023819
373.555	3.99678	0.63218	0.353796
372.554	3.91709	0.67524	0.336123
368.064	3.57951	0.77293	0.265302
363.069	3.23529	0.83853	0.215609
358.084	2.91864	0.88789	0.180897
353.086	2.62773	0.92916	0.154415
288.262	0.48990	1.24291	0.023809
308.179	0.88678	1.16730	0.043353

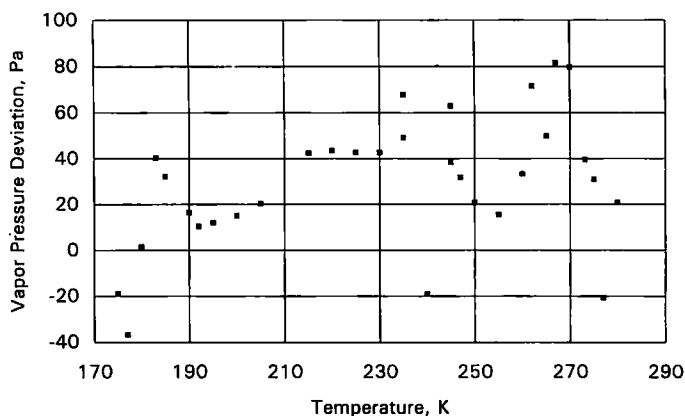
Fig. 3. Deviations $p_{\text{meas}} - p_{\text{cal}}$ of measured vapor pressures from vapor pressures calculated with the fundamental equation [2].

Table II. Experimental (p, ρ, T) Data for R134a

T_{90} (K)	p (MPa)	ρ ($\text{kg} \cdot \text{dm}^{-3}$)
180.031	0.90967	1.56369
180.516	1.59395	1.56329
181.022	2.34570	1.56293
181.510	3.03886	1.56257
182.039	3.79724	1.56218
182.606	4.60857	1.56176
190.047	0.97380	1.53732
190.517	1.60450	1.53696
191.222	2.54798	1.53644
191.526	2.94384	1.53622
191.528	2.94683	1.53622
192.005	3.57809	1.53588
192.507	4.24631	1.53551
192.685	4.49182	1.53539
200.034	0.86150	1.51090
200.997	2.05951	1.51021
201.517	2.70622	1.50984
202.017	3.33418	1.50949
202.534	3.96305	1.50915
203.026	4.59455	1.50881
200.076	0.97322	1.51106
201.015	2.13214	1.51037
201.509	2.73273	1.51002
201.800	3.08713	1.50981
202.122	3.48269	1.50958
202.483	3.93290	1.50933
202.908	4.46677	1.50903
210.036	0.91545	1.48255
210.576	1.55196	1.48219
211.499	2.61395	1.48155
212.304	3.55114	1.48101
212.810	4.14998	1.48070
212.998	4.37268	1.48060
220.034	0.91180	1.45500
220.502	1.42198	1.45469
221.506	2.50927	1.45404
222.505	3.59900	1.45342
222.902	4.03810	1.45319
223.303	4.47562	1.45295
230.015	0.98161	1.42707
230.500	1.48172	1.42679
231.503	2.49431	1.42618
232.498	3.51082	1.42560
233.001	4.02808	1.42533

Table II. (Continued)

T_{90} (K)	p (MPa)	ρ (kg · dm ⁻³)
233.500	4.54142	1.42506
240.031	0.75981	1.39767
240.525	1.22875	1.39738
241.557	2.20307	1.39680
242.541	3.15406	1.39628
243.264	3.83529	1.39590
243.991	4.52411	1.39551
249.999	0.76340	1.36808
250.503	1.21108	1.36782
251.513	2.08699	1.36726
252.821	3.24241	1.36659
253.658	3.98695	1.36618
254.125	4.40802	1.36598
260.033	1.00634	1.33824
260.747	1.59765	1.33790
261.736	2.41170	1.33741
262.721	3.22047	1.33695
263.702	4.02686	1.33648
264.190	4.42375	1.33626
264.196	4.42964	1.33626

Table III. The Vapor Pressure of R134a Between 175 and 280 K

T_{90} (K)	p (MPa)	Coefficients of Eq. (3) for 175 < T < 280 K
174.980	0.00066	$A = -7.5333021$
177.020	0.00080	$B = 1.4448575$
180.001	0.00113	$C = -2.1538915$
190.015	0.00284	$D = -4.0370148$
192.005	0.00335	$T_{90,cr} = 374.18$ K [2]
195.032	0.00429	$p_{cr} = 4.056$ MPa [2]
200.033	0.00634	
205.013	0.00915	
215.099	0.01808	
219.998	0.02447	
225.008	0.03283	
230.003	0.04334	
235.002	0.05644	
235.023	0.05652	

Table III. (Continued)

T_{90} (K)	p (MPa)	Coefficients of Eq. (3) for $175 < T < 280$ K
239.995	0.07244	
245.000	0.09212	
245.002	0.09211	
246.999	0.10100	
249.997	0.11562	
255.004	0.14373	
260.010	0.17694	
262.001	0.19173	
265.017	0.21586	
266.980	0.23284	
270.003	0.26093	
273.154	0.29288	
275.013	0.31312	
276.998	0.33585	
279.965	0.37228	

ACKNOWLEDGMENT

The investigations of the thermodynamic properties in the liquid region were supported by the Deutsche Forschungsgemeinschaft.

REFERENCES

1. R. Tillner-Roth, Forsch.-Ber. DKV Nr. 41 (Deutscher Kälte- und Klimatechnischer Verein, Stuttgart, 1993).
2. R. Tillner-Roth and H. D. Baehr, *J. Phys. Chem. Ref. Data* **23**:657 (1994).
3. A. E. Elhassan and K. M. de Reuck, *Preliminary Report on Equations of State for Environmentally Acceptable Refrigerants* (IUPAC Thermodynamic Tables Project Centre, Imperial College, London, 1992).
4. A. E. Elhassan, R. J. B. Craven, and K. M. de Reuck, *Comparisons of Equations of State with Experimental Data for R134a and R123* (IUPAC Thermodynamic Project Tables Centre, London, 1993).
5. S. G. Penoncello, R. T. Jacobsen, R. C. Williams, and E. W. Lemmon, *Equation of State Comparisons for HFC-134a and HCFC-123* (University of Idaho, Moscow, 1993).
6. M. Fukushima, *Trans. JAR* **8**:65 (1991).
7. M. L. Huber and J. F. Ely, *Int. J. Refrig.* **15**:393 (1992).
8. Y. Maezawa, H. Sato, and K. Watanabe, *J. Chem. Eng. Data* **35**:225 (1990).
9. M. O. McLinden, J. S. Gallagher, L. A. Weber, G. Morrison, D. K. Ward, A. R. H. Goodwin, M. R. Moldover, J. W. Schmidt, H. B. Chae, T. J. Bruno, J. F. Ely, and M. L. Huber, *ASHRAE Trans.* **95**:263 (1989).

10. C. Yokoyama and S. Takahashi, *Fluid Phase Equil.* **67**:227 (1991).
11. W. Wagner, K. Brachthäuser, R. Kleinrahm, and H. W. Lössch, *Int. J. Thermophys.* **16**:399 (1995).
12. W. Blanke and R. Weiss, *Fluid Phase Equil.* **80**:179 (1992).
13. A. K. Bandyopadhyay, W. Blanke, and J. Jäger, *PTB-Mitt.* **101**:269–274 (1991).
14. W. Wagner, personal communication (1986).